Bio-based substances from urban waste as auxiliaries for solar photo-Fenton treatment under mild conditions: optimization of operational variables

J. Gomis[1], L. Carlos[2], A. Bianco Prevot[3], A. C. S. C. Teixeira[4], M. Mora[5], A.M. Amat[1], R. Vicente[1], A. Arques[1*].

(1) Grupo de Procesos de Oxidación Avanzada, Dpto de Ingeniería Textil y Papelera, Universitat Politècnica de València. Plaza Ferrándiz y Carbonell s/n, Alcoy, Spain. aarques@txp.upv.es.

(2) Instituto de Investigaciones Fisicoquímicas Teóricas y Aplicadas (INIFTA), CCT-La Plata-CONICET, Universidad Nacional de La Plata, Diag 113 y 64, La Plata, Argentina.

(3) Dipartimento di Chimica, Università di Torino, Via Giuria 7, Torino, Italy.

(4) Escola Politécnica da Universidade de São Paulo, Av. Prof. Luciano Gualberto, tr.3, 380, São Paulo, Brasil.

(5) Dpto de Matemática Aplicada, Universitat Politècnica de València. Plaza Ferrándiz y Carbonell s/n, Alcoy, Spain.

*Corresponding author: mail: aarques@txp.upv.es, phone: ++34 966528417

Abstract

The use of soluble bio-based organic substances (SBO) obtained from urban wastes to expand the pH region where the photo-Fenton process can be applied has been

investigated in this study. For this purpose, a mixture of six pollutants, namely acetaminophen, carbamazepine, amoxicillin, acetemiprid, clofibric acid and caffeine, at an initial concentration of 5 mg L^{-1} each, has been employed. Surface response methodology, based on the Doehlert matrix, has shown to be a useful tool to determine the effect of pH (in the range 3-7), concentration of SBO (15-25 mg L^{-1}) and iron (2-6 mg L^{-1}) on the performance of the photodegradation of the studied pollutants, measured by their half-life. Results indicate that, at high SBO concentration, the optimum pH shifts in most cases to a higher value (between 3 and 4) and that a significant loss of efficiency of the process was only observed at pH values above 5. An iron concentration of 4-5 mg L^{-1} and an amount of SBO of 19-22 mg L^{-1} have been determined to be the optimal conditions for the degradation of most of the studied pollutants at pH = 5.

Graphical abstract

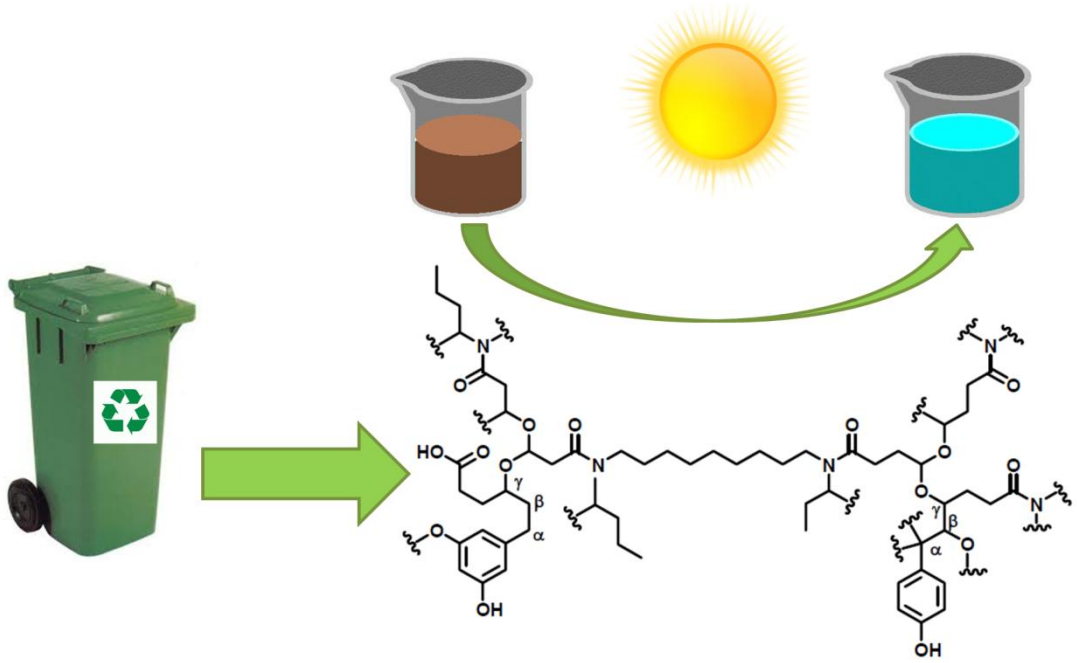

Highlights

The effect of operational variables on the photo-Fenton process has been studied.

Surface response methodology has been applied for this purpose.

Soluble bio-organic substances enable an efficient photo-Fenton at higher pH

Keywords

Photo-Fenton, emerging pollutants, pH, soluble organic matter, SBO

1. Introduction

Wastes have deserved attention from researchers, as they could be a sustainable source of materials with a wide range of potential applications [1]. In particular, soluble bio-based organic substances (SBO) have been isolated from solid organic wastes submitted to aging under aerobic fermentation conditions, following a process that involves extraction of the soluble fraction at basic pH and posterior precipitation at acidic media [2]. SBO are constituted by a mixture of macromolecules, which average molecular weight ranges from 67 to 463 kg mol^{-1}; they consist of long aliphatic chains, aromatic rings and several oxygen and nitrogen-containing functional groups [2]. Hence, these materials show basic structural similarities with some macromolecules found in natural organic matter (NOM), such as humic and fulvic acids, which play an important role in

photochemical processes leading to the self-remediation of ecosystems [3]. In this context, determining the potential use of SBO for water detoxification is meaningful, as this may be considered a green process since it valorises solid wastes as sources of photoactive materials with similar properties as less available NOM. Information on this issue is very scarce, and only some recent papers have been published reporting on the ability of these compounds to act as photocatalysts in the degradation of chlorophenols [4, 5], sulphonic acids [6], dyes [7, 8] or pharmaceuticals [9]. SBOs action can be related to an enhanced photogeneration of reactive species; however, the strong screen effect produced by these coloured materials negatively affects the degradation of pollutants that can undergo direct photolysis. When simulated sunlight was employed as irradiation source, the screen effect becomes predominating, thus making SBOs unattractive as solar photocatalysts [9].

Alternatively, SBOs might also be employed as complexing agents to drive photo-Fenton processes at mild conditions. Photo-Fenton is based on the ability of iron salts to catalyse decomposition of hydrogen peroxide into highly oxidizing species (mainly hydroxyl radicals, although other species might also contribute) in a process that is accelerated by irradiation [10]. One major drawback of this process is the highly acidic media required to avoid formation of non-active iron oxides or hydroxides. However, some efforts have been recently made for the implementation of photo-Fenton at circumneutral pH. This approach might be especially useful to treat emerging pollutants (EPs) as a certain loss of efficiency in the generation of reactive species might be acceptable in this case, as EPs are commonly found at low concentration, and hence lesser amounts of oxidizing species are necessary [11, 12]. This strategy can be improved by using chemical auxiliaries, able to form photoactive complexes, at mild

pH, with the iron added [13]. Humic acids are among the materials employed for this purpose, because of their ability for iron complexation [13-16].

Because of their similarity with humic substances, SBOs are also candidates to extend the application of photo-Fenton to pH conditions where iron ions are normally not soluble. Indeed, photo-Fenton process in the presence of SBOs have been recently shown to be able to remove a mixture of EPs at pH=5.2 [9]. Hence, a logical step beyond is to determine the role of the operational parameters on the efficiency of the process. For this purpose, a response surface methodology based on Doehlert design has been chosen in this work in order to determine the effect of SBOs and iron concentrations at the pH interval between 3, close to the optimal value, and 7. The Doehlert design has been commonly employed as a chemometric tool, enabling to minimize the number of experiments required to obtain the surface [17, 18]. The mixture of EPs employed in previous work [9, 16] has been chosen as target solution: acetaminophen, carbamazepine, amoxicillin, acetamiprid, clofibric acid and caffeine (see Figure 1 for structures).

2. Experimental

2.1 Reagents

Acetaminophen, caffeine, amoxicillin, clofibric acid, carbamazepine and acetamiprid were purchased from Sigma-Aldrich and used as received. Hydrogen peroxide (30% v/v), ferric chloride, sulphuric acid and sodium hydroxide, were obtained from Panreac. Water was Milli-Q grade.

The SBO employed in this work, namely CVT230, was obtained from urban biowastes supplied by ACEA Pinerolese waste treatment plant (Pinerolo, Italy) following a procedure detailed elsewhere [2, 19]. Briefly, the starting material was compost from gardening-park trimming residues matured for 230 days: it was digested 4 h at 60 °C at alkaline conditions (pH = 13) and 4 V/w water/solid ratio to favour hydrolysis of organics. Alkaline hydrolyzed solution have been recognized as very similar to the humic matter, in turn characterized by the presence of a dimensionally smaller fraction (fulvic acid) soluble in all the pH range, and of a bigger one (humic acid), not soluble below pH 3. Instead of separating the two fractions by means of pH variation, the size difference was exploited. The recovered liquid phase was therefore circulated through a polysulfone ultrafiltration membrane with 5 kD molecular weight cut-off to yield a retentate with 5-10 % dry matter content. The membrane retentate was dried at 60 °C to yield the final water soluble bio-based product (SBO). It contained 72.1% (w/w) of volatile solids and the carbon content was 38.3 % (see [8] for further details).

2.2 Reactions

Experiments were performed in a 250 mL cylindrical Pyrex vessel irradiated with a solar simulator (Sun 2000, ABET Technologies) equipped with a 550 W Xenon Short Arc Lamp. A pyrex glass filter was used to cut off radiation below 300 nm (which only accounted for a residual fraction of the lamp irradiance). The vessel was loaded with an aqueous solution containing the six EPs at an initial concentration of 5 mg L^{-1} each. SBO concentration was varied in the range 15-25 mg L^{-1}; $FeCl_3$ was added to reach a concentration of iron between 2 and 6 mg L^{-1}. The initial amount of hydrogen peroxide

131 was 2.2 mmol L^{-1} in all cases, which is half the stoichiometric amount required to
132 mineralize the EPs; this concentration was employed in order to obtain a relatively slow
133 kinetics, which allows a better determination and comparison of illumination times
134 required to remove the EPs under the different conditions that have been studied. The
135 pH was adjusted to the desired value (3-7) by dropwise addition of either 0.1 mmol L^{-1}
136 NaOH or 0.1 mmol L^{-1} H_2SO_4. Temperature was kept in the range 30-35 ºC throughout
137 the reaction. Samples were periodically taken from the solution, filtered through a
138 polypropylene membrane (0.45μm) and diluted 1:1 with methanol.

139

140 Control experiments showed that direct photolysis of the pollutants was negligible
141 under the employed conditions and irradiation in the presence of H_2O_2 solely resulted in
142 a moderate degradation of amoxicillin (less than 20% after 200 min of irradiation).

143

144 2.3. Analysis

145 The concentration of each EP was determined by UPLC (Perkin Elmer model Flexar
146 UPLC FX-10). A Brownlee Analytical column (DB-C18) was employed as stationary
147 phase. The eluent consisted in a mixture of acetonitrile (A) and a 0.1% formic acid
148 aqueous solution (B); the relative amount of each solvent was changed following a
149 linear gradient, from 3% A to 70% A in 8 min; the flow rate was 0.3 mL min^{-1}.
150 Detection wavelengths were 205 nm (acetaminophen, amoxicillin, caffeine and
151 carbamazepine), 225 nm (clofibric acid) and 245 nm (acetamiprid). Identification and
152 quantification of the EPs were performed by comparison with standards.

153

154 2.4 Surface response methodology

155

156 In order to gain further insight into the effect of the studied operational variables (pH,
157 SBO and iron concentration), an experimental design methodology based on a Doehlert
158 array [20]. In this case, a total of 15 experiments (k^2+k+1, where k is the number of
159 analysed variables, 3 in this study, plus two replicates of the central point) were
160 performed. Experimental conditions of all experiments are found in Table 1. The
161 software Statgraphics Centurion XVI was used for response surface model fitting by
162 means of the least squares method. The illumination time required to degrade each
163 pollutant to 50% of its initial concentration ($t_{50\%}$) was used as response, which was
164 obtained from the plot of the relative EP concentration vs. illumination time.

165

166 **3. Results and discussion**

167

168 Plots of the relative concentration of each EP vs illumination time were obtained for
169 each experiment (see Figure 2 for an example). Considering an illumination time of 90
170 minutes, the results show complete removal of all EPs for the experiments carried out at
171 pH 3. At pH 5, removals between 90 and 100% were obtained for all EPs except
172 acetamiprid, for which removals in the range 54-68.5% were obtained. These results
173 confirm the efficiency of the photo-Fenton reaction under acidic and mildly acidic
174 conditions, the later favoured by the presence of SBOs. Finally, maximum percent
175 removals between 5.7 and 64.7% were obtained for the experiments carried out at pH 7,
176 again the lowest removals after 90 minutes of illumination (5.7-21%) corresponding to
177 acetamiprid. These trends show that the choice of a response like the illumination time

178 necessary to obtain pollutant removals of 90% or greater could not be considered for all
179 EPs and pH for the conditions used in the present study (pollutants initial
180 concentrations, H_2O_2 and iron concentrations) and in some cases would require too long
181 illumination times to be observed.

182

183 As a result, the illumination time required for the removal of 50% of each pollutant
184 ($t_{50\%}$) was considered for every experiment (Table 1). From the practical point of view,
185 the response $t_{50\%}$ is not submitted to phenomena such as lack of hydrogen peroxide or
186 changes in the experimental conditions that can affect the kinetic behaviour and/or
187 reproducibility (mainly under the less efficient conditions, where too long illumination
188 times would be required. Based on the response values in Table 1, six three-dimensional
189 full quadratic response surface models were obtained, one for each EP (see Table 2,
190 Equations I-A to I-F). For all EPs the values of the determination coefficient (R^2) were
191 high (92.4; 97.4; 98.1; 97.1; 95.9; and 99.4% for amoxicillin, carbamazepine,
192 acetamiprid, clofibric acid, caffeine, and acetaminophen, respectively), indicating good
193 agreement between experimental and calculated values of the response variable. In each
194 case, the values of the residuals (differences between calculated and measured values of
195 $t_{50\%}$) as a function of measured values were randomly distributed with error zero with
196 zero mean.

197

198 The corresponding ANOVA tables (see Supplementary Data, Tables T1-T6) and the
199 Pareto charts (Figure 3) show that except for acetaminophen, the only significant effect
200 on $t_{50\%}$ at 95% confidence level (p-values < 0.05) was due to pH, as expected, being the
201 reaction faster at lower pH values; the quadratic effect of this variable was significant,

indicating the important curvature of the response surfaces. For acetaminophen, the quadratic effect of SBO concentration was also significant. Therefore, simplified model equations for $t_{50\%}$ were fitted by considering the effect of pH only, as presented in Table 2 (cf. Equation II-A to II-F) (see Supplementary Data, Tables T7-T12 for the corresponding ANOVA tables). In comparison with the complete model equations, in most cases the values of R^2 decreased as the simplified fitted models exhibit lack-of-fit and fail to predict $t_{50\%}$ for the experiments in which the effects of SBO and Fe(III) concentrations on the response are important (see Supplementary Data, Figures F1-F6). In other words, the effect of pH on the response is so pronounced that it masks the effects of the other variables, especially that of SBO concentrations for some pH conditions. For that reason, in order to discuss some trends concerning the effects of SBO and Fe(III) concentrations and to better determine the pH domain where the photo-Fenton could be applied, the complete fitted response surface models were considered, and two-dimensional contour plots were built for each EP by fixing [SBO] at the higher and lower values.

Figure 4A shows data obtained for carbamazepine. At low SBO concentration, a fast decrease in the efficiency of photo-Fenton with increasing pH is observed, as the line corresponding to $t_{50\%}$ = 20 min can be found at a pH of ca. 4 and that of 60 min at a pH of approximately 5.5. At low pH (below 4) an increase in [Fe(III)] results in a slight enhancement of the process. This behaviour could be attributed to differences in iron availability: at acidic medium, higher amounts of iron can be kept in solution, what results in a faster degradation reaction; however, above pH = 4, SBOs are not able to prevent efficiently iron precipitation and reaction rate decreases.

In contrast, at the highest SBO concentration (25 mg L^{-1}) a different trend can be found: the loss of efficiency of the process occurs at higher pH, as differences are not acute in the pH range 3-5.5, what suggests that SBOs are useful materials to apply the photo-Fenton reaction at milder pH conditions. Furthermore, the optimum pH shifted to higher values (ca. 4). This might indicate a change in the photo-Fenton mechanism, in which the key species is not only $Fe(OH)^{2+}$ (responsible for the optimal pH value of 2.8), but photoactive iron-SBO complexes might also contribute. Modification of the optimum pH has already been described when species able to modify iron complexation are present. For instance, at high concentration of chloride, photo-Fenton exhibits the best performance at a pH slightly above 3 [21]. In addition, changes in photo-Fenton mechanism at circumneutral values and or in the presence of chelating agent, such as EDTA [22, 23] or citrate [24, 25], have been proposed, eventually changing the key species [26]. Interestingly, when ethylenediamine-N,N'-disuccinic acid (EDDS) was used as complexing agent, best results were reached at neutral or even slightly basic medium; this variation was attributed to a completely different mechanism in which superoxide plays a key role [27]. In the case of SBOs, experiments carried out with chemical probes have shown that other species, in addition to •OH radicals, are responsible for pollutants degradation [8-9].

Results obtained with clofibric acid (Figure 4E) and caffeine (Figure 4F) are very similar to carbamazepine and for these compounds the photo-Fenton reaction showed to be efficient until pH slightly above 5 at [SBO] of 25 mg L^{-1}. In fact, previous experiments involving mild photo-Fenton conditions with non-complexed iron or in the presence of humic substances or SBOs have demonstrated that they follow similar behaviour with only quantitative differences. Acetamiprid (Figure 4D) is the most

252 recalcitrant compound towards the photo-Fenton process [8, 9]. This low reactivity
253 results in a poor efficiency of photo-Fenton, which quickly decreases with increasing
254 pH (the line of $t_{50\%}$ = 60 is at pH ca. 5 at low and high SBO concentrations).
255 Amoxicillin, on the other hand, is the most reactive among the EPs towards photo-
256 Fenton and at [SBO] = 25 mg L^{-1} shows the highest efficiency at pH = 5 and reaction
257 rate did not decrease significantly until values close to 7 (Figure 4C). Finally, for
258 acetominophen (Figure 4B) a slow but continuous decrease in reaction rate with
259 increasing pH is observed (line $t_{50\%}$ = 60 min at pH = 6). In fact, in a previous study [9]
260 this compound has been shown to have a different reactivity in comparison to the other
261 EPs, in which other species than •OH play an important role.

262

263 Based on those results, it could be hypothesised that the presence of SBOs modifies the
264 photo-Fenton mechanism and, although some differences in the individual behaviour of
265 each EP have been evidenced, the process can be extended, in most cases, at least up to
266 pH = 5. Hence it is interesting to determine at this pH value the role of [Fe(III)] and
267 [SBO] in view of optimizing these variables. Contour plots obtained at pH = 5 for all six
268 EPs can be observed in Figure 5; the corresponding fitted equations are shown in Table
269 2 (cf. Table 2, Equations III-A to III-F) (see Supplementary Data for the ANOVA
270 tables, Tables T13-T18). In general, an optimum can be found in the region 4-5 mg L^{-1}
271 of iron and 19-22 mg L^{-1} of SBO, which should be considered as the best conditions for
272 the removal of the EPs from water by the photo-Fenton process. Under those conditions,
273 $t_{50\%}$ was ca. 20 min for all EPs, except for amoxicillin ($t_{50\%}$ < 10 min) and for
274 acetamiprid, which was the most refractory; in fact, acetamiprid was the only compound
275 which did not show a minimum for $t_{50\%}$ in the studied region.

276

277 The behaviour of SBO can be explained by considering that this species is necessary to
278 keep iron in solution and to allow the photo-Fenton process at pH = 5. However, beyond
279 a given point the role of SBO might be detrimental because it can act as scavenger of
280 the reactive species, competing with the pollutants, or because of a light screening effect
281 related to its brown colour. In the case of iron, it seems that amounts above 4 mg L^{-1}
282 play a negative role; this can be attributed to the faster precipitation of iron to form
283 oxides/hydroxides, which, in turn, decrease the photo-Fenton efficiency.

284

285 **Conclusions**

286

287 SBOs have been demonstrated as useful materials to allow the implementation of the
288 photo-Fenton processes at higher pH values (at least 5). This can be due to the ability of
289 these materials to complex iron, thus avoiding its precipitation as oxides or hydroxides.
290 The surface response methodology enabled to study the effect of iron, SBO and pH on
291 the process. Surface responses obtained at pH = 5 showed that optimal conditions of
292 Fe(III) and SBO concentrations were in the range 4-5 mg L^{-1} and 19-22 mg L^{-1}
293 respectively. Extending this methodology to other variables (e.g. H_2O_2 concentration) or
294 other compounds is a logical step forward.

295

296 Although a mechanistic study for such a complex system falls beyond the aim of this
297 study, our results seem to point to a modification of the photo-Fenton mechanism in
298 which the optimum pH shifts to higher values (in most cases in the range 3-4, slightly
299 above the optimal value described for photo-Fenton, 2.8). Furthermore, some
300 differences in the behaviour of each EP have been identified, which may be explained

by their reactivity with the new species formed, whose nature remains to be elucidated. Hence, further research on the mechanistic issues of the process seems meaningful.

Finally, future work is also required to study the process at pH = 5 under real sunlight at pilot plant with more realistic aqueous matrixes, estimating values such as H_2O_2 consumption, irradiation time or changes in biocompatibility, in order to better assess the real applicability of this methodology.

Acknowledgements

The authors want to thank the financial support of the European Union (PIRSES-GA-2010-269128, EnvironBOS) and Spanish Ministerio de Educación y Ciencia (CTQ2012-38754-C03-02). Juan Gomis would like to thank UPV for his FPI grant (2010-07).

References

[1] R.A.D. Arancon, C.S.K. Lin, K.M. Chan, T.H.Kwan, R. Luque, Energy Sci. Technol, 1 (2013) 53-71.

[2] E. Montoneri, D. Mainero, V. Boffa, D.G. Perrone, C Montoneri, Int J. Global Environ. Issues 11 (2011) 170-196.

[3] S. K. Khetan, T.J. Collins, Chem. Rev. 107 (2007) 2319-2364.

[4] A. Bianco Prevot, P. Avetta, D. Fabbri, E. Laurenti, T. Marchis, D.G. Perrone, E. Montoneri, V. Boffa, ChemSusChem 4 (2011) 85-90.

323 [5] P. Avetta, F. Bella, A. Bianco Prevot, E. Laurenti, E. Montoneri, A. Arques, L.
324 Carlos, Sustainable Chem. Eng. 1 (2013) 1545-1550.

325 [6] P. Avetta, A. Bianco Prevot, D. Fabbri, E. Montoneri, L. Tomasso, L. Chem. Eng. J.
326 197 (2012) 193-198.

327 [7] A. Bianco Prevot, D. Fabbri, E. Pramauro, C. Baiocchi, C. Medana, E. Montoneri,
328 V. Boffa, J. Photochem. Photobiol. A: Chem. 209 (2010) 224-231.

329 [8] J. Gomis, R.F. Vercher, A.M. Amat, D.O. Martire, M.C. González, A. Bianco-
330 Prevot, E. Montoneri, A. Arques, L. Carlos. Catal. Today, 209 (2013) 176-180.

331 [9] J. Gomis, A. Bianco Prevot , E. Montoneri, M.C. González, A.M. Amat, D.O.
332 Mártire, A. Arques, L. Carlos, Chem. Eng. J. 235 (2014) 236-243.

333 [10] J.J. Pignatello, E. Oliveros, A. MacKay, Critical Rev. Environ. Sci. Technol. 36
334 (2006) 1-84.

335 [11] I. Carra, J.L. Casas López, L. Santos-Juanes, S. Malato, J.A. Sánchez Pérez, Chem
336 Eng. J. 224 (2013) 67-74.

337 [12] N. De la Cruz, L. Esquius, D. Grandjean, A. Magnet, A. Tungler, L.F. de
338 Alencastro, C. Pulgarin. Water Res. 47 (2013) 5836-5845.

339 [13] N. Klamerth, S. Malato, A. Agüera, A. Fernández-Alba. Water Res. 47 (2013) 833-
340 840.

341 [14] N. Klamerth, S. Malato, M.I. Maldonado, A. Agüera, A. Fernández-Alba, Catal.
342 Today 161 (2011) 241-246.

343 [15] A. Bernabeu, R.F.Vercher, L.Santos-Juanes, P.J.Simón, C.Lardín, M.A.Martínez,
344 J.A. Vicente, R.González, C.Llosá, A.Arques, A.M. Amat, Catal. Today, 161 (2011)
345 235-240.

346 [16] A. Bernabeu, S. Palacios, R.Vicente, R. Vercher, S.Malato, A. Arques, A.M. Amat.
347 Chem Eng. J. 198-199 (2012) 65-72.

348 [17] D.H. Doehlert. Uniform shell designs. J R Stat Soc.,Ser C 19 (1970) 231–239.

349 [18] M.A. Bezerra, R.E. Santelli, E.P. Oliveira, L.S.Villar, L.A. Escaleira, Talanta 76
350 (2008) 965–977.

351 [19] Montoneri E., Boffa V., Savarino P., Perrone D.G., Ghezzo M., Montoneri C.,
352 Mendichi R., Waste Manage. 31 (2011) 10-17

353 [20] S. L. C. Ferreira, W. N. L. dos Santos, C. M. Quintella, B. B. Neto, J. M. Bosque-
354 Sendra, Talanta 63 (2004) 1061-1067.

355 [21] A. Machulek, J.E.F. Moraes, C. Vautier-Giongo, C.A. Silverio, L.C. Friedrich,
356 C.A.O. Nascimento, M.C. González, F Quina, Environ. Sci. Technol. 41 (2007) 8459–
357 8463.

358 [22] N. Klamerth, S. Malato, A. Agüera, A. Fernández-Alba, G. Mailhot, Environ. Sci.
359 Technol. 46 (2012) 2885-2892.

360 [23] J.D. Rush, W.H. Koppenol, J. Biol. Chem. 261 (1986), 6730-6733.

361 [24] M.R.A. Silva, A.G. Trovó, R.F.P. Nogueira, J. Photochem. Photobiol A: Chem.
362 191 (2007) 187-192

363 [25] H. Katsumata, S. Kaneco, T. Suziki, K. Ohta, Y. Yobiko, J. Photochem. Photobiol
364 A: Chem.180 (2006) 38-45.

365 [26] S.J. Hug, O. Leupin, Environ. Sci. Technol. 37 (2003), 2734-2742.

366 [27] W. Huang, M. Brigante, F. Wu, C. Mousty, K. Hanna, G. Mailhot, Environ. Sci.

367 Technol. 47 (2013) 1952-1959

368

Exp number	[Fe(III)]	[SBO]	pH	A	B	C	D	E	F
1	4	20	5	21.6	25.8	14.4	57.6	24.3	25.5
1’	4	20	5	18.1	24.9	16	54.1	24.6	26.6
1’’	4	20	5	15	22	10	48.8	20.4	23.2
2	6	20	5	23.8	26.6	12.8	59.5	28.2	31.3
3	5	25	5	27.8	33.8	22	68.9	32.1	36.4
4	2	20	5	27.9	28.4	24.4	57	29.5	35.1
5	3	15	5	34.4	41.6	26.3	83.9	40.3	47.1
6	5	15	5	33.3	36.4	24.4	68.9	36.1	39.6
7	3	25	5	27.5	33	22.3	65.8	33.7	35.8
8	5	21.7	7	129.4	86.3	111.5	320	133.3	207.5
9	3	21.7	7	88.4	82.1	62.4	218	87.4	109.7
10	4	16.7	7	154	75.5	174.3	242.7	156.4	150
11	3	18.3	3	2.3	3.3	2.3	6.4	2.7	3.1
12	5	18.3	3	1.7	1.5	1	3.9	2.1	1.8
13	4	23.3	3	1.3	2.4	1.3	4.6	1.8	2.1

Table 1: Experimental points used to obtain the response surface (Doehlert matrix). The concentrations of SBO and iron are expressed as mg L^{-1}; data given in the last six columns correspond to the time (in min) required to decrease concentration of each EP to 50% of the initial value for carbamazepine (A), acetaminophen (B), amoxicillin (C), acetamiprid (D), clofibric acid (E) and caffeine (F)

Compound	Equation
Carbamazepine	$t_{50\%}$ (min) = 248.38 – 40.37·[Fe] – 8.52·[SBO] – 51.39·pH + 1.90·$[Fe]^2$ + 0.07 [Fe] [SBO] + 5.14·[Fe]·pH + 0.43 $[SBO]^2$ – 2.08·[SBO]·pH + 10.28·pH^2 (R^2 = 0.974) (I-A) $t_{50\%}$ (min) = 106.29 – 62.86 pH + 9.34 pH^2 (R^2 = 0.915) (II-A) $t_{50\%}$ (min) = 239.50 – 17.38·[Fe] – 17.88 [SBO] + 1.90 $[Fe]^2$ + 0.43 $[SBO]^2$ + 0.07 [Fe] [SBO] (R^2 = 0.930) (III-A)
Acetominophen	$t_{50\%}$ (min) = 318.33 – 15.36·[Fe] – 22.79·[SBO] – 32.82·pH + 0.82·$[Fe]^2$ + 0.30 [Fe] [SBO] + 0.50 [Fe] pH + 0.45 $[SBO]^2$ + 0.71·[SBO]·pH + 3.64·pH^2 (R^2 = 0.994) (I-B) $t_{50\%}$ (min) = 3.98 – 9.21 pH + 2.89 pH^2 (R^2 = 0.963) (II-B) $t_{50\%}$ (min) = 253.57 – 13.20·[Fe] – 19.60 [SBO] + 0.82 $[Fe]^2$ + 0.45 $[SBO]^2$ + 0.3 [Fe] [SBO] (R^2 = 0.972) (III-B)
Amoxicillin	$t_{50\%}$ (min) = 56.92 – 41.63·[Fe] + 3.80·[SBO] – 19.34·pH + 1.28·$[Fe]^2$ + 0.08 [Fe] [SBO] + 6.23·[Fe]·pH + 0.36 $[SBO]^2$ – 4.19·[SBO]·pH + 10.69·pH^2 (R^2 = 0.924) (I-C) $t_{50\%}$ (min) = 123.65 – 70.42 pH + 9.91 pH^2 (R^2 = 0.794) (II-C) $t_{50\%}$ (min) = 199.27 – 13.98·[Fe] – 15.04 [SBO] + 1.28 $[Fe]^2$ + 0.36 $[SBO]^2$ + 0.08 [Fe] [SBO] (R^2 = 0.879) (III-C)
Acetamiprid	$t_{50\%}$ (min) = 966.42 – 83.28·[Fe] – 40.02·[SBO] – 206.76·pH + 1.19·$[Fe]^2$ + 0.91·[Fe]·[SBO] + 12.29·[Fe]·pH+ 0.69·$[SBO]^2$ + 1.77·[SBO]·pH + 18.59·pH^2 (R^2 = 0.981) (I-D) $t_{50\%}$ (min) = 180.38 – 110.88 pH + 17.47 pH^2 (R^2 = 0.946) (II-D) $t_{50\%}$ (min) = 440.30 – 28.18·[Fe] – 32.03 [SBO] + 1.19 $[Fe]^2$ + 0.69 $[SBO]^2$ + 0.91 [Fe] [SBO] (R^2 = 0.915) (III-D)
Clofibric acid	$t_{50\%}$ (min) = 242.78 – 40.30·[Fe] – 9.39·[SBO] – 44.58·pH + 1.44·$[Fe]^2$ + 0.13 [Fe] [SBO] + 5.70·[Fe]·pH + 0.44 $[SBO]^2$ – 2.06·[SBO]·pH + 9.40·pH^2 (R^2 = 0.971) (I-E) $t_{50\%}$ (min) = 88.28 – 54.22 pH + 8.51 pH^2 (R^2 = 0.907) (II-E) $t_{50\%}$ (min) = 246.10 – 14.80·[Fe] – 18.67 [SBO] + 1.44 $[Fe]^2$ + 0.44 $[SBO]^2$ + 0.13 [Fe] [SBO] (R^2 = 0.955) (III-E)
Caffeine	$t_{50\%}$ (min) = 702.53 – 79.39·[Fe] – 25.36·[SBO] – 147.13·pH + 2.02·$[Fe]^2$ + 0.41 [Fe] [SBO] + 12.04·[Fe]·pH + 0.50·$[SBO]^2$ + 0.65 [SBO] pH + 12.44·pH^2 (R^2 = 0.959) (I-F) $t_{50\%}$ (min) = 126.86 – 75.73 pH + 11.41 pH^2 (R^2 = 0.890) (II-F) $t_{50\%}$ (min) = 310.83 – 25.51·[Fe] – 22.51 [SBO] + 2.03 $[Fe]^2$ + 0.50 $[SBO]^2$ + 0.41 [Fe] [SBO] (R^2 = 0.984) (III-F)

Table 2: Response surface models obtained for each EP, where the values of the variables are specified in their original units. (I) refer to the complete fitted model, (II) to the simplified fitted model without the non-significant variables, and (III) to the fitted model considering only the experiments performed at pH 5

381 Figure 1: Chemical structures of EPs used in this study

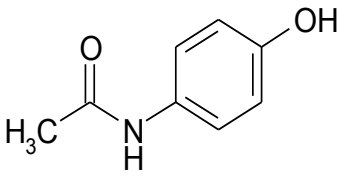

Acetominophen

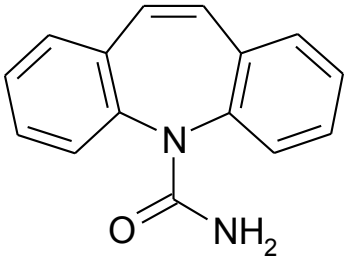

Carbamazepine

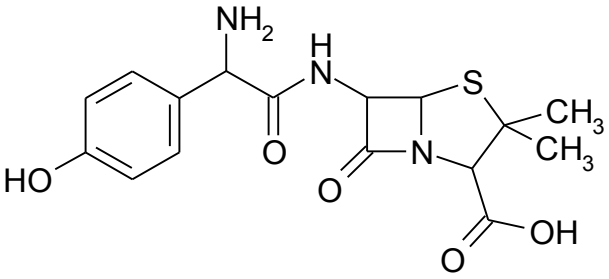

Amoxicillin

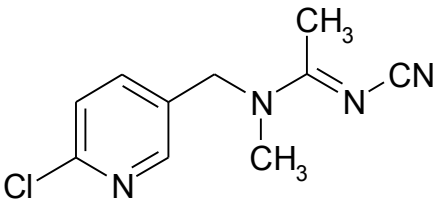

Acetamiprid

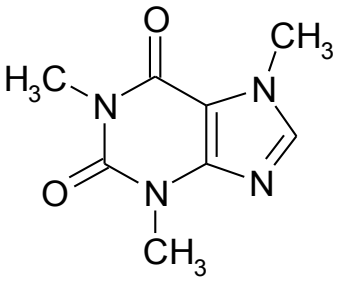

Caffeine

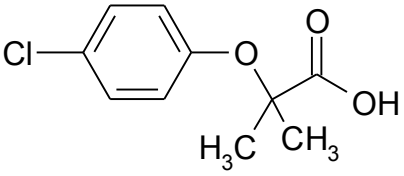

Clofibric acid

382 Figure 2: Example of the photodegradation of a mixture of 6 EPs by means of the
383 photo-Fenton reaction. Plot of the relative concentration vs time: amoxicillin (▲),
384 acetaminophen (●), acetamiprid (×), caffeine (□), clofibric acid (♦) and carbamazepine
385 (◊). Data correspond to the central point ([SBO] = 20 mg L^{-1}, [Fe(III)] = 4 mg L^{-1}, pH =
386 5)

387

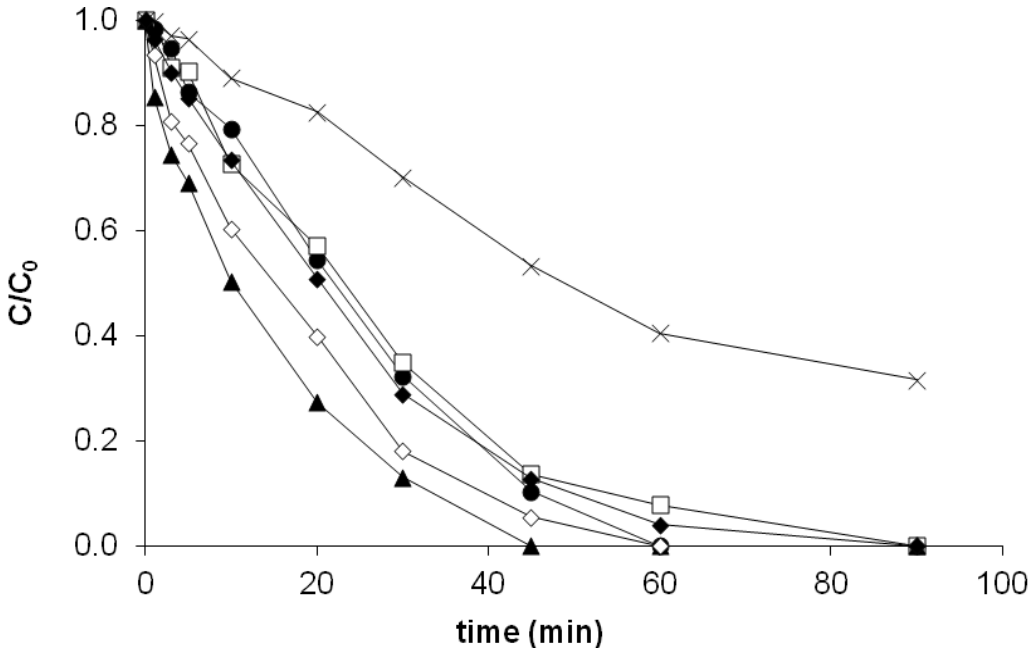

388

389

Figure 3: Pareto charts for the response $t_{50\%}$ (min) obtained for the photo-Fenton degradation of EPs in the presence of SBO. The EPs are carbamazepine (A), acetaminophen (B), amoxicillin (C), acetamiprid (D), clofibric acid (E) and caffeine (F)

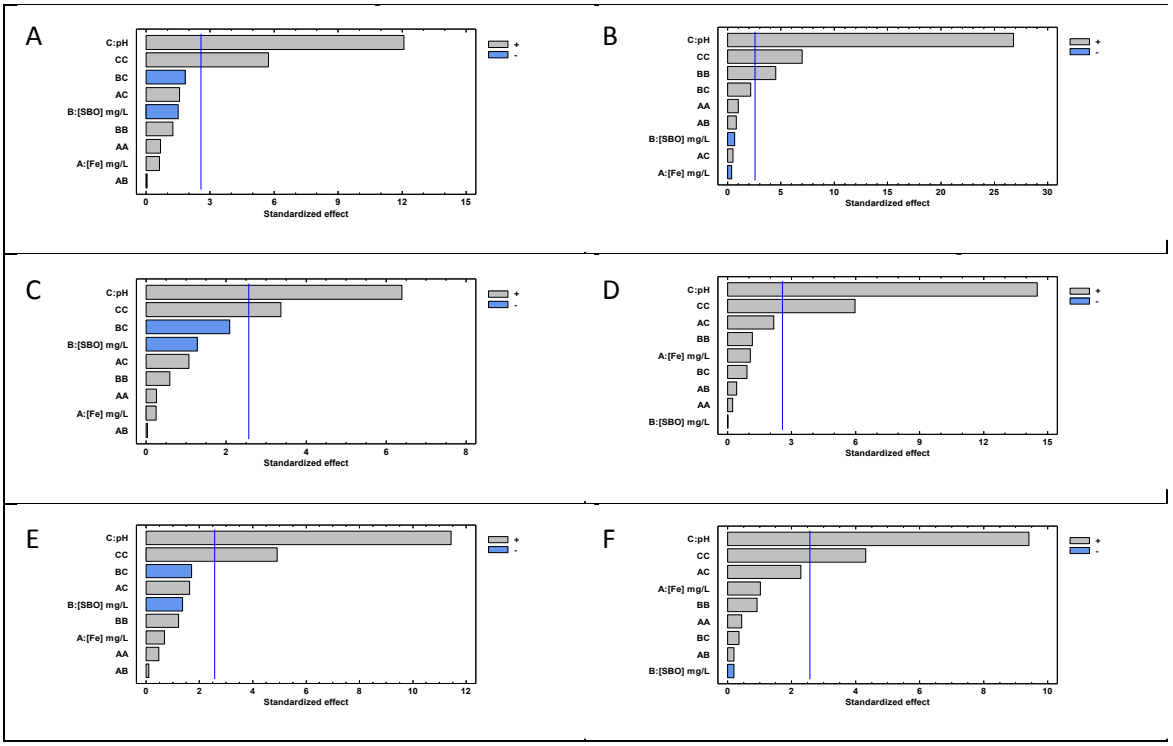

394

395 Figure 4: Contour plots for $t_{50\%}$ (min) obtained for the photo-Fenton degradation of EPs

396 in the presence of SBO. The EPs are carbamazepine (A), acetaminophen (B),

397 amoxicillin (C), acetamiprid (D), clofibric acid (E) and caffeine (F)

398

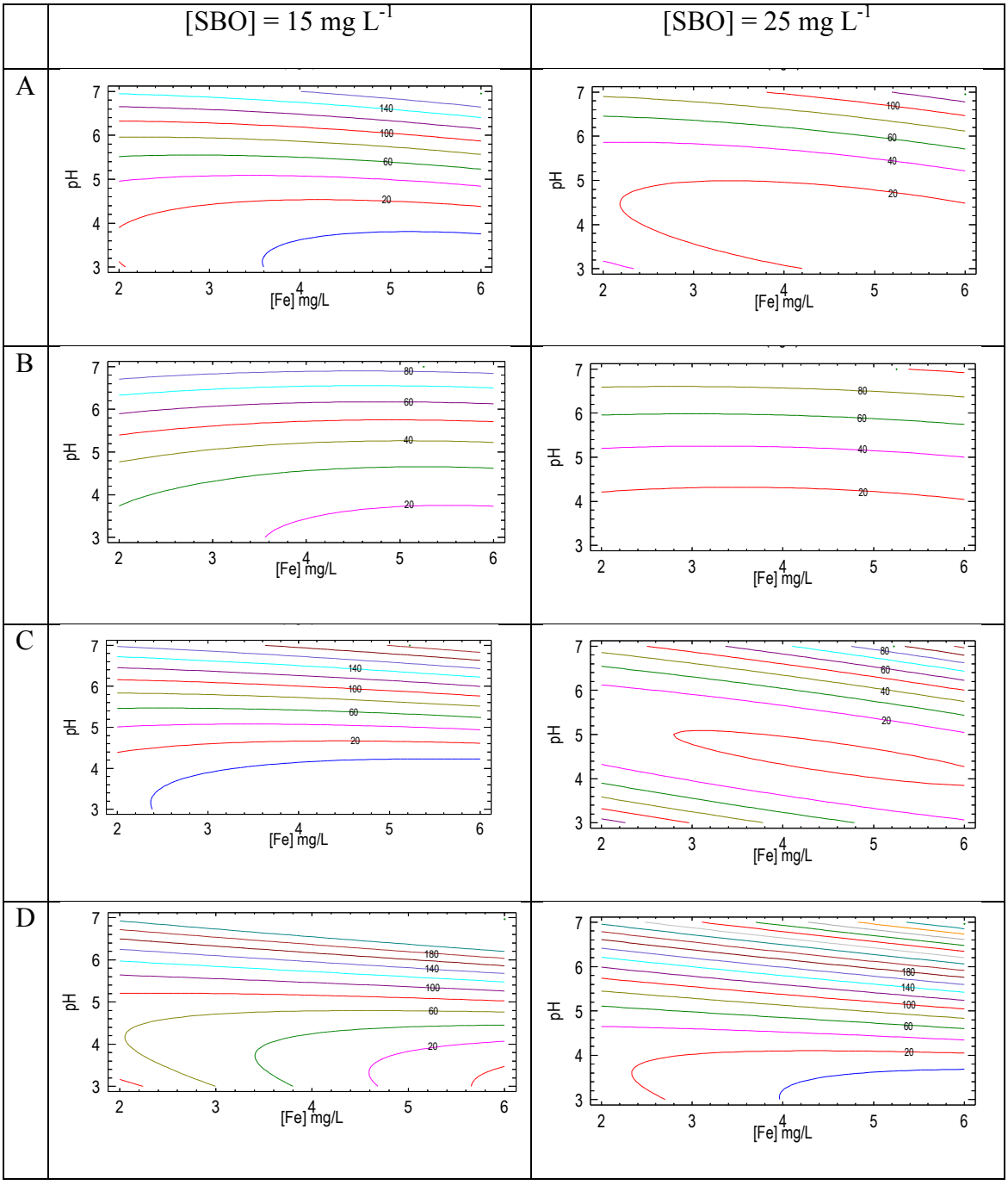

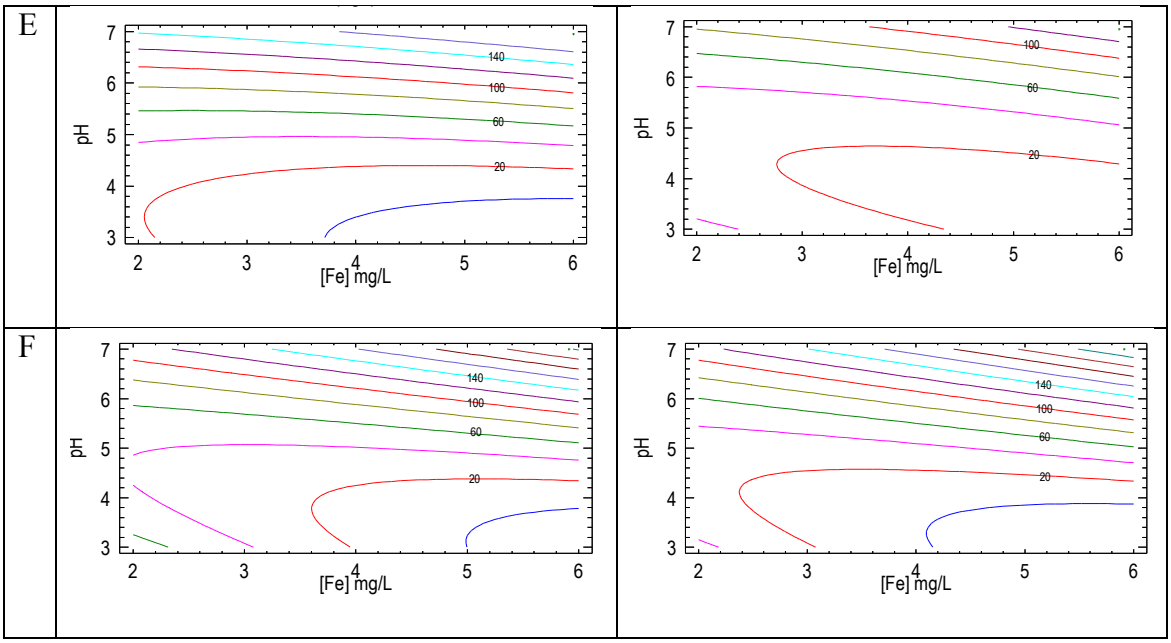

399

400

401

402

403 Figure 5: Contour plots for $t_{50\%}$ (min) obtained for the photo-Fenton degradation of EPs

404 at pH = 5. The EPs are carbamazepine (A), acetaminophen (B), amoxicillin (C),

405 acetamiprid (D), clofibric acid (E) and caffeine (F)

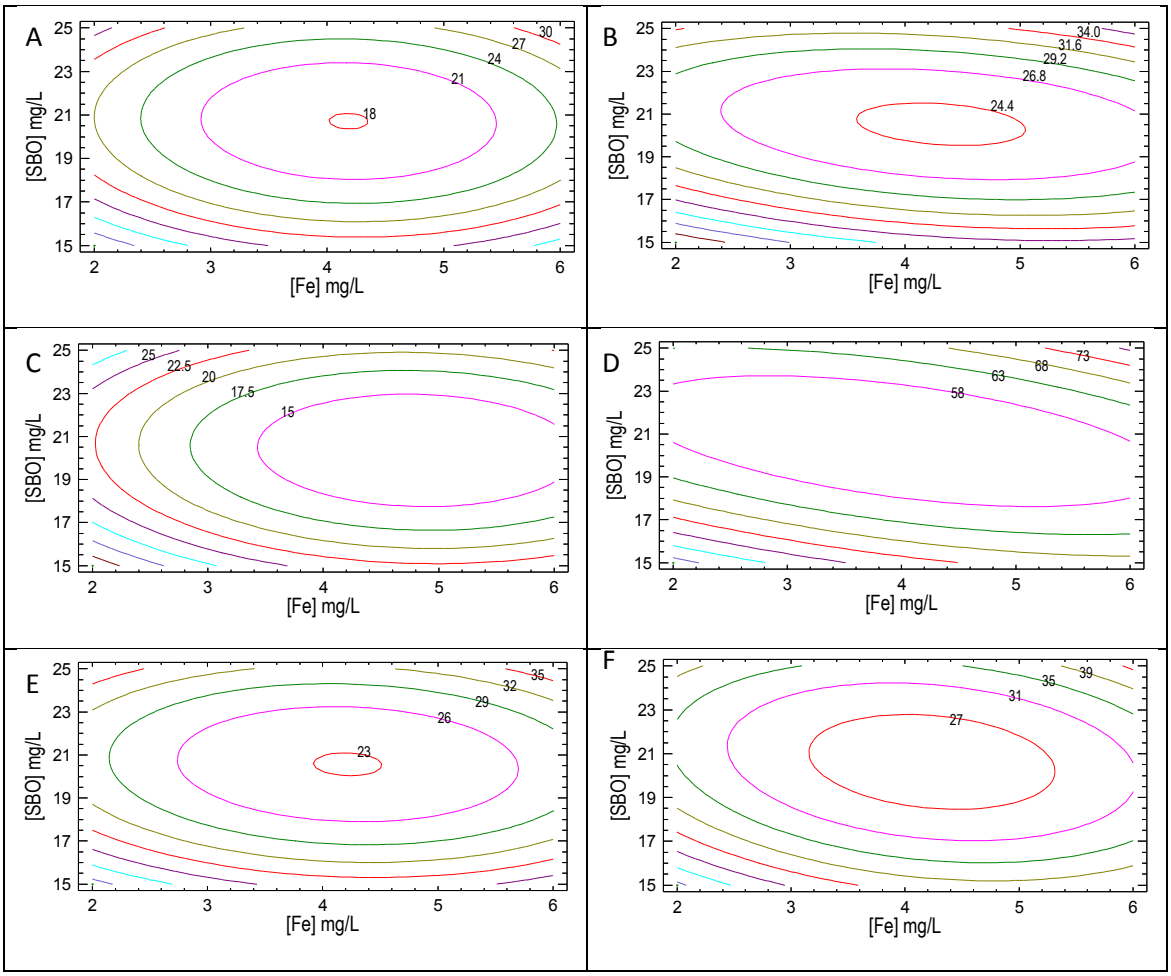

406

e-component

Click here to download e-component: supplementary data.docx